JOURNAL OF MODERN OPTICS, 2002, VOL. 49, NO. 13, 2129–2152

A transfer matrix approach to local field calculations in multiple-scattering problems

BRIAN STOUT

Institut Fresnel, Unité Mixte de Recherche associée au CNRS 6133, Case 262, Faculté des Sciences et Techniques, Centre de Saint Jérome, 13397 Marseille Cedex 20, France; e-mail: brian.stout@fresnel.fr

JEAN-CLAUDE AUGER

Centro de Investigacion en Polimeros, COMEX, Marcos Achar Logaton 2, 55885 Tepexpan, Estado de México

and JACQUES LAFAIT

Laboratoire d'Optique des Solides, l'Université Pierre et Marie Curie, Unité Mixte de Recherche associée au CNRS 7601, Case 80, 4 place Jussieu 75252 Paris Cedex 05, France

(*Received 23 July 2001; revision received 12 December 2001*)

Abstract. We present a new recursive transfer matrix method for calculating local electromagnetic fields in systems of spheres subject to strong dependent scattering. Local field information is often lost or discarded in recursive transfer matrix approaches. In order to preserve the local field information, and to avoid problems associated with the dimensional cut-off of the translation matrices, we calculate the scatterer-centred transfer matrices. Our technique permits systematic studies of local field effects for all possible incident field directions, and configurations (including orientation averages). Illustrative calculations are presented.

1. Introduction

Recent years have seen considerable developments in the calculations of strong dependent multiple scattering. A natural tool for such calculations is the translation–addition theorem, in which the coefficients of a spherical wave expansion about a given point are multiplied by translation–addition matrices which transform them into coefficients of a spherical partial wave expansion around a different origin. Such infinite matrix multiplications have numerical applications only because there exists a natural cut-off in the problem. Indeed, for a particle of a given size in a medium of wave-vector amplitude k, only partial waves up to certain finite order can significantly interact with the particle. A conservative estimate of the cut-off for spheres of radius R is given (as a function of kR) by the Wiscombe [1] criteria.

Although one can rather readily write down the multiple-scattering equations, the large number of unknowns and the sparse nature of the equations, often prevents a direct matrix inversion solution for three-dimensional systems [2–5].

Journal of Modern Optics ISSN 0950–0340 print/ISSN 1362–3044 online
http://www.tandf.co.uk/journals
DOI: 10.1080/09500340210124450

Consequently, most calculations in the literature have been of an iterative nature. In applications, however, it is frequently advantageous to calculate the transfer matrix for the multiple scattering system. One of the advantages of the transfer matrix approach is that it contains, once and for all, the information concerning all possible incident field configurations, directions and polarizations. This more complete information concerning the scattering system is particularly useful when carrying out the orientation averages often necessary when treating macroscopic transport phenomenon.

Several researchers have proposed the calculation of cluster transfer matrices, $\mathbf{T}_N^{\mathrm{cl}}$, via constructive approaches which build the transfer matrix of a complete system through successive (recursive) steps [3, 6]. Each of these individual steps is calculationally less demanding than the full matrix inversion of the equations of the entire system. A major obstacle in these recursive approaches is that they suffer from a growth in the number of dimensions of the partial wave basis beyond that necessary to describe individual scatterings, as recently discussed by Siqueira and Sarabandi [4]. A second important lack of these new transfer matrix approaches is that, in practice, one often loses (or discards) local field information. This loss of information is of no importance (and often considered desirable) if one is interested only in far field quantities (e.g. total cross-sections). However, there is increasing interest in the local field enhancements which can occur in multiple-scattering systems, and it can prove useful to keep this information in the transfer matrix formalism.

In this work, we demonstrate a recursive technique which carries out the matrix inversion of the complete system of equations in a numerically reliable manner, while avoiding any undesirable 'growth' of the partial wave dimensions beyond that necessary to describe the individual scatterings. Our attention is concentrated on systems of impenetrable spheres. In such systems, the multiple-scattering formulation contains the necessary information for determining the entire local field configuration.

The outline of this work is as follows. Section 2 consists of an introduction to the formalism via a reminder of some of the basic definitions of partial wave expansions, incident and scattered fields, and the individual transfer matrices. These definitions permit compact derivations of multiple-scattering theory. Section 3, then contains a brief review of multiple scattering theory and serves to familiarize the reader with our notation. In section 4, we develop a recursive procedure for constructing the scatterer-centred transfer matrices $\mathbf{T}_N^{(i,j)}$. It will be shown that working with the $\mathbf{T}_N^{(i,j)}$ allows the dimensional cut-off to be brought under control. In section 5, we present formulae for obtaining useful physical information such as orientation fixed and orientation averaged cross sections. We also derive, in this section, formulae for extracting local field information. In section 6, we present some illustrative results for cross sections, and fields in the interiors of the scatterers of strongly scattering three-dimensional systems. We make our concluding remarks in section 7.

2. Spherical wave expansions and individual transfer matrices

An incident field $\mathbf{E}_{\mathrm{i}}$ impinging on an N-particle system can be developed in terms of regular spherical waves developed about some point $\mathbf{0}$ chosen as the origin of the system of scatterers (figure 1):

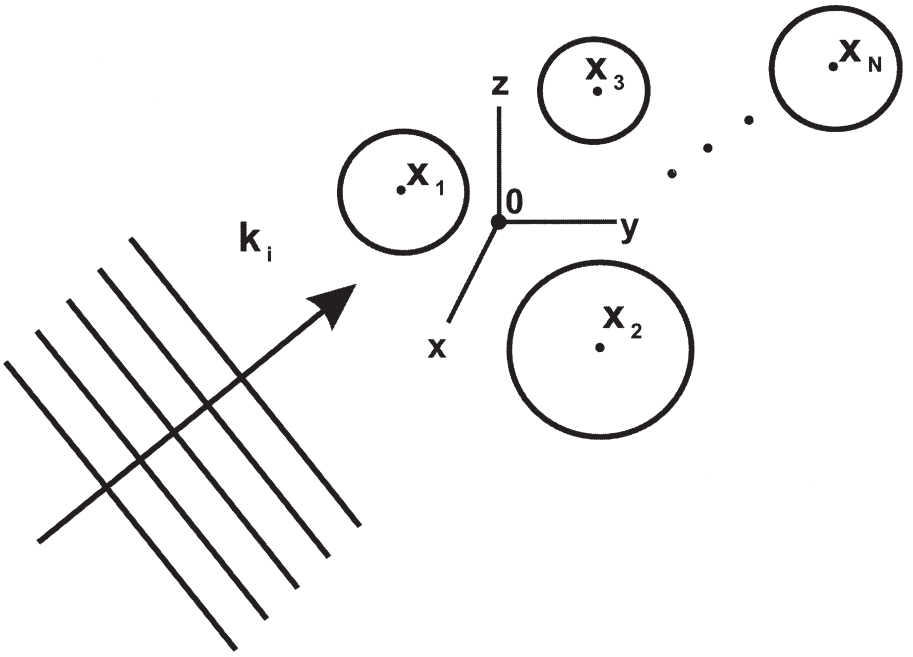

Figure 1. A two-dimensional projection of a system of multiple light scattering by spheres. A field is incident on the system with a wave-vector $\mathbf{k_i}$. The centres of the spheres are denoted $\mathbf{x}_j$, $j = 1, \ldots, N, N$ being the number of spheres in the system.

$$\begin{aligned}\mathbf{E}_{\mathrm{i}}(\mathbf{r}) &= E\sum_{n=1}^{\infty}\sum_{m=-n}^{n}[\mathcal{R}g\{\mathbf{M}_{nm}(k\mathbf{r})\}\mathrm{a}_{nm}^{\mathbf{M}} + \mathcal{R}g\{\mathbf{N}_{nm}(k\mathbf{r})\}\mathrm{a}_{nm}^{\mathbf{N}}] \\ &= E[\mathcal{R}g\{\mathbf{M}(k\mathbf{r})\},\ \mathcal{R}g\{\mathbf{N}(k\mathbf{r})\}]\cdot\begin{bmatrix}\mathrm{a}^{\mathbf{M}}\\ \mathrm{a}^{\mathbf{N}}\end{bmatrix} \\ &\equiv E\mathcal{R}g\{\boldsymbol{\mathcal{E}}^{\mathrm{t}}(k\mathbf{r})\}\cdot\mathbf{a}, \end{aligned} \tag{1}$$

where $\mathbf{M}_{nm}$ and $\mathbf{N}_{nm}$ are the vector spherical waves (see appendix A), and E is a real parameter which determines the field amplitude of the incident wave. In the second line, the troublesome summation over multipolarity indices has been suppressed by invoking a matrix notation wherein the indices n and m label the components in an abstract vector space [7]. The column vector $\mathbf{a}$ is composed of the incident field coefficients. In the last line, the notation is simplified still further by defining $\boldsymbol{\mathcal{E}}(k\mathbf{r})$ as an abstract vector composed of the vector wavefunctions $\mathbf{M}(k\mathbf{r})$ and $\mathbf{N}(k\mathbf{r})$. The superscript t stands for the transpose of a column vector into a row vector. The notation $\mathcal{R}g\{\ \ \}$ stands for 'the regular part of' [7] (see appendix A).

It is also possible to describe scattered fields via spherical wave expansions. In a multiple-scattering system, the total field $\mathbf{E}_{\mathrm{t}}^{\mathrm{cl}}(\mathbf{r})$ outside the scatterers is simply the sum of the incident and scattered fields:

$$\mathbf{E}_{\mathrm{t}}^{\mathrm{cl}}(\mathbf{r}) = \mathbf{E}_{\mathrm{i}} + \mathbf{E}_{\mathrm{s}}^{\mathrm{cl}}(\mathbf{r}). \tag{2}$$

It is practical to develop the scattered field around the particle centres. The centre of the jth particles will henceforth be denoted by $\mathbf{x}_j$, and the spherical coordinates relative to each scatterer are written $\mathbf{r}_j = \mathbf{r} - \mathbf{x}_j$. The scattered field $\mathbf{E}_{\mathrm{s}}^{(j)}$ emanating from the jth particle can be developed in terms of outgoing spherical waves (see appendix A, equations (A 4)) in the coordinates of the respective centre. The coefficients of this development are denoted by the scattering vector $\mathbf{f}^{(j)}$. The scattered field of the entire cluster can thus be expressed

$$\mathbf{E}_{\mathrm{s}}^{\mathrm{cl}}(\mathbf{r}) = \sum_{j=1}^{N} \mathbf{E}_{\mathrm{s}}^{(j)}(\mathbf{r}_j) = E \sum_{j=1}^{N} \boldsymbol{\mathcal{E}}^{\mathrm{t}}(k\mathbf{r}_j) \cdot \mathbf{f}^{(j)}. \tag{3}$$

A central concept in developing a multiple-scattering theory is that of an excitation field for the individual particles. In an N-particle cluster, the excitation field $\mathbf{E}_{\mathrm{e}}^{(j)}$ for a particle j is generated by the incident field and the (multiple) scattering of the incident field by remaining $N-1$ scatterers.

In a spherical basis developed around its respective centre, an excitation field can be developed in terms of the regular spherical waves:

$$\mathbf{E}_{\mathrm{e}}^{(j)}(\mathbf{r}) = E\mathcal{R}g\{\boldsymbol{\mathcal{E}}^{\mathrm{t}}(k\mathbf{r}_j)\} \cdot \mathbf{e}^{(j)}. \tag{4}$$

A final and central definition necessary to the formulation of a multiple scattering theory is the one-body transfer matrices $\mathbf{T}_1^{(j)}$, which yield the scattering coefficients $\mathbf{f}^{(j)}$ in terms of the coefficients of the excitation field impinging on the jth scatterer:

$$\mathbf{f}^{(j)} \equiv \mathbf{T}_1^{(j)} \cdot \mathbf{e}^{(j)}. \tag{5}$$

For a sphere, $\mathbf{T}_1^{(j)}$ is a diagonal matrix whose elements are given by the Mie [8] coefficients [9, 10].

3. Multiple-scattering theory for clusters

3.1. *Theory of the excitation field*

Formally at least, the equations of multiple scattering theory are relatively easily derived. By definition, the excitation field (or locally incident field) $\mathbf{E}_{\mathrm{e}}^{(j)}(\mathbf{r})$ for the jth particle in the cluster is the sum of the incident field, and the field scattered by all of the remaining particles, that is

$$\begin{aligned}\mathbf{E}_{\mathrm{e}}^{(j)}(\mathbf{r}) &\equiv \mathbf{E}_{\mathrm{i}}(\mathbf{r}) + \sum_{l=1,l\neq j}^{N} \mathbf{E}_{\mathrm{s}}^{(l)}(\mathbf{r}) \\ &= E\mathcal{R}g\{\boldsymbol{\mathcal{E}}^{\mathrm{t}}(k\mathbf{r})\} \cdot \mathbf{a} + E \sum_{l=1,l\neq j}^{N} \boldsymbol{\mathcal{E}}^{\mathrm{t}}(k\mathbf{r}_l) \cdot \mathbf{f}^{(l)}.\end{aligned} \tag{6}$$

Using the translation–addition theorem (appendix B), this field may be rewritten as a regular field expansion around the centre of the corresponding particle

$$\mathbf{E}_{\mathrm{e}}^{(j)}(\mathbf{r}_j) = E\mathcal{R}g\{\boldsymbol{\mathcal{E}}^{\mathrm{t}}(k\mathbf{r}_j)\} \cdot \boldsymbol{\beta}^{(j,0)} \cdot \mathbf{a} + E \sum_{l=1,l\neq j}^{N} \mathcal{R}g\{\boldsymbol{\mathcal{E}}^{\mathrm{t}}(k\mathbf{r}_j)\} \cdot \boldsymbol{\alpha}^{(j,l)} \cdot \mathbf{f}^{(l)}, \tag{7}$$

where $\boldsymbol{\alpha}^{(j,l)} \equiv \boldsymbol{\alpha}(\mathbf{x}_j - \mathbf{x}_l)$ is the irregular translation matrix in the notation of Chew [3] (see appendix B) and the dots $(\cdot)$ indicate that we have made a matrix multiplication over the spherical wave components.

Invoking the definition of the excitation field coefficients (equation (4)), equation (7) can be written entirely in terms of the field cofficients, that is

$$\mathbf{e}^{(j)} = \boldsymbol{\beta}^{(j,0)} \cdot \mathbf{a} + \sum_{l=1, l\neq j}^{N} \boldsymbol{\alpha}^{(j,l)} \cdot \mathbf{f}^{(l)}. \tag{8}$$

Using the definition of the one-body transfer matrix (equation (5)), one obtains a set of N coupled matrix equations with the excitation coefficients as the unknowns:

$$\mathbf{e}^{(j)} = \boldsymbol{\beta}^{(j,0)} \cdot \mathbf{a} + \sum_{l=1, l\neq j}^{N} \boldsymbol{\alpha}^{(j,l)} \cdot \mathbf{T}_1^{(l)} \cdot \mathbf{e}^{(l)}. \tag{9}$$

We regard this equation as the fundamental multiple-scattering equation from which all the solutions considered here may be formulated. It is important to keep in mind that $\mathbf{e}^{(j)}$ and $\mathbf{a}$ are in principal infinite-dimensional vectors. Numerical solutions to equation (9) are only possible because the matrix elements of the one-body transfer matrix are essentially zero beyond a certain multipolarity order $n_{\max}$. Consequently, nearly exact analytic solutions to equation (9) can be obtained by working within a basis set truncated to contain all multipolarity orders up to $n_{\max}$. Taking into account the axial 'quantum' numbers m (see equation (1) and appendix B), the truncated dimension L of the vectors $\mathbf{e}^{(j)}$ and $\mathbf{a}$ is $L = 2n_{\max}^2 + 4n_{\max}$.

3.2. *Scatterer-centred cluster transfer matrices*

Once an appropriate cut-off dimension $n_{\max}$ has been applied, the most direct method to solve for the $\mathbf{e}^{(j)}$ is to arrange the N equations of equation (9) as a $(NL \times NL)$-dimensional 'system' matrix and to solve for the $\mathbf{e}^{(j)}$ by matrix inversion:

$$\begin{bmatrix} \mathbf{e}^{(1)} \\ \mathbf{e}^{(2)} \\ \vdots \\ \mathbf{e}^{(N)} \end{bmatrix} = \begin{bmatrix} \mathbf{I} & -\boldsymbol{\alpha}^{(1,2)} \cdot \mathbf{T}_1^{(2)} & \cdots & -\boldsymbol{\alpha}^{(1,N)} \cdot \mathbf{T}_1^{(N)} \\ -\boldsymbol{\alpha}^{(2,1)} \cdot \mathbf{T}_1^{(1)} & \mathbf{I} & \cdots & -\boldsymbol{\alpha}^{(2,N)} \cdot \mathbf{T}_1^{(N)} \\ \vdots & \vdots & \ddots & \vdots \\ -\boldsymbol{\alpha}^{(N,1)} \cdot \mathbf{T}_1^{(1)} & -\boldsymbol{\alpha}^{(N,2)} \cdot \mathbf{T}_1^{(2)} & \cdots & \mathbf{I} \end{bmatrix}^{-1} \begin{bmatrix} \boldsymbol{\beta}^{(1,0)} \cdot \mathbf{a} \\ \boldsymbol{\beta}^{(2,0)} \cdot \mathbf{a} \\ \vdots \\ \boldsymbol{\beta}^{(N,0)} \cdot \mathbf{a} \end{bmatrix}, \tag{10}$$

where $\mathbf{I}$ denotes the identity matrix. This equation can be expressed in terms of the scattering vectors $\mathbf{f}^{(j)}$ by multiplying both sides of the above equation by a block diagonal matrix composed of the one-body transfer matrices:

$$\begin{bmatrix} \mathbf{T}_1^{(1)} & 0 & \cdots & 0 \\ 0 & \mathbf{T}_1^{(2)} & \cdots & 0 \\ \vdots & \vdots & \ddots & \vdots \\ 0 & 0 & \cdots & \mathbf{T}_1^{(N)} \end{bmatrix}. \tag{11}$$

Using equation (5) on the left-hand side, equation (10) then takes the form

$$\begin{bmatrix} \mathbf{f}^{(1)} \\ \mathbf{f}^{(2)} \\ \vdots \\ \mathbf{f}^{(N)} \end{bmatrix} \equiv \begin{bmatrix} \mathbf{T}_N^{(1,1)} & \mathbf{T}_N^{(1,2)} & \cdots & \mathbf{T}_N^{(1,N)} \\ \mathbf{T}_N^{(2,1)} & \mathbf{T}_N^{(2,2)} & \cdots & \mathbf{T}_N^{(2,N)} \\ \vdots & \vdots & \ddots & \vdots \\ \mathbf{T}_N^{(N,1)} & \mathbf{T}_N^{(N,2)} & \cdots & \mathbf{T}_N^{(N,N)} \end{bmatrix} \begin{bmatrix} \boldsymbol{\beta}^{(1,0)} \cdot \mathbf{a} \\ \boldsymbol{\beta}^{(2,0)} \cdot \mathbf{a} \\ \vdots \\ \boldsymbol{\beta}^{(N,0)} \cdot \mathbf{a} \end{bmatrix}. \tag{12}$$

This procedure thereby defines the scatterer-centred transfer matrices $\mathbf{T}_N^{(j,k)}$. The $\mathbf{T}_N^{(j,k)}$ matrices form a complete multiple-scattering solution of the entire N-particle system. Following Mackowski [5], this system of equations can be compactly expressed as

$$\mathbf{f}^{(j)} = \sum_{k=1}^{N} \mathbf{T}_N^{(j,k)} \cdot \boldsymbol{\beta}^{(k,0)} \cdot \mathbf{a}. \tag{13}$$

Although formally simple, the above method of obtaining $\mathbf{T}_N^{(j,k)}$ is often impractical for three-dimensional systems of spheres owing to the numerical difficulties in inverting the matrix in equation (10).

4. Transfer matrix constructions

An alternative to the direct matrix inversion outlined in section 3.2 is to formulate the solution in terms of individual transfer matrices $\mathbf{T}_N^{(j)}$ (defined in section 4.1 below). Like the scatterer-centred transfer matrices $\mathbf{T}_N^{(j,k)}$ of equation (9), these matrices retain local field information. The property of $\mathbf{T}_N^{(j)}$ of principal interest to us is that they can be obtained via computationally efficient recursive techniques. Section 4.2 is essentially a review of a recursive approach of a type proposed by Chew [3]. The dimensional problems associated with this technique are also described in this section. Finally, in section 4.3, we show how the dimensionality problems can be eliminated by adapting the recursive technique to calculate the scatterer-centred cluster transfer matrices $\mathbf{T}_N^{(j,k)}$.

4.1. *Individual* N*-body transfer matrices*

In an N-body cluster, an individual transfer matrix $\mathbf{T}_N^{(j)}$ yields the coefficients of the field scattered by the jth particle in terms of the incident field, while taking into account the multiple scattering from all other scatterers. The $\mathbf{T}_N^{(j)}$ are thus defined such that

$$\begin{aligned} \mathbf{f}^{(j)} &\equiv \mathbf{T}_N^{(j)} \cdot \boldsymbol{\beta}(k\mathbf{x}_j) \cdot \mathbf{a} \\ &\equiv \mathbf{T}_N^{(j)} \cdot \boldsymbol{\beta}^{(j,0)} \cdot \mathbf{a}, \end{aligned} \tag{14}$$

where the $\boldsymbol{\beta}^{(j,0)}$ factor was introduced in order for $\mathbf{T}_N^{(j)}$ to be independent of the choice of system origin. There is a close relationship between the matrices $\mathbf{T}_N^{(j)}$ and $\mathbf{T}_N^{(j,k)}$, as we will show later in equation (27).

A system of matrix equations for the $\mathbf{T}_N^{(j)}$ is readily obtained from the basic multiple-scattering equatiions by inserting the definition of $\mathbf{T}_N^{(j)}$ into the excitation field coefficient equation (8):

$$\mathbf{e}^{(j)} = \boldsymbol{\beta}^{(j,0)} \cdot \mathbf{a} + \sum_{l=1,l\neq j}^{N} \boldsymbol{\alpha}^{(j,l)} \cdot \mathbf{T}_N^{(l)} \cdot \boldsymbol{\beta}^{(l,0)} \cdot \mathbf{a}. \tag{15}$$

An equation for the scattered field coefficients is obtained by multiplying both sides of this equation by $\mathbf{T}_1^{(j)}$. Invoking equation (5) and the group properties of the regular translation matrices yields

$$\mathbf{f}^{(j)} = \mathbf{T}_1^{(j)} \cdot \left(\mathbf{I} + \sum_{l=1,l\neq j}^{N} \boldsymbol{\alpha}^{(j,l)} \cdot \mathbf{T}_N^{(l)} \cdot \boldsymbol{\beta}^{(l,j)} \right) \cdot \boldsymbol{\beta}^{(j,0)} \cdot \mathbf{a}. \tag{16}$$

Finally, invoking the definition of the N-body transfer matrices (equation (14)), gives N equations for the N unknown $\mathbf{T}_N^{(j)}$ matrices:

$$\mathbf{T}_N^{(j)} = \mathbf{T}_1^{(j)} \cdot \left(\mathbf{I} + \sum_{l=1,l\neq j}^{N} \boldsymbol{\alpha}^{(j,l)} \cdot \mathbf{T}_N^{(l)} \cdot \boldsymbol{\beta}^{(l,j)} \right). \tag{17}$$

This equation may be regarded as the fundamental equation for the individual transfer matrices. Although the $\mathbf{T}_N^{(j)}$ may in principle be solved iteratively (see, for example, [11]), the presence of regular translation matrices $\boldsymbol{\beta}^{(l,j)}$ on the far right-hand side of equation (17) introduce dimensionality problems associated with multiplying truncated translation matrices. Putting this problem aside for the moment, we review in the next section an efficient recursive method for obtaining these matrices [3].

4.2. *Recursive solutions for* $\mathbf{T}_N^{(j)}$

Recursive solutions are in principle an efficient means of calculating the $\mathbf{T}_N^{(j)}$ matrices. One assumes that the scattering problem of $N-1 \geqslant 1$ particles is known and with this knowledge solve the N-body problem. Since the one-body solution for a sphere is known, the solution for any finite cluster is obtained recursively.

In the recursive method, the new particle added to the system is labelled N. The formal solution (equation (17)) obtained above yields an equation for this scatterer, that is

$$\mathbf{T}_N^{(N)} = \mathbf{T}_1^{(N)} \cdot \left(\mathbf{I} + \sum_{l=1}^{N-1} \boldsymbol{\alpha}^{(j,l)} \cdot \mathbf{T}_N^{(l)} \cdot \boldsymbol{\beta}^{(l,j)} \right). \tag{18}$$

In order to create a recursive system, a second equation is needed. Following the work by Chew [3], $\mathbf{E}_{N-1,\mathrm{cl}}^{(j)}$ is defined as the excitation field of the jth particle in the $(N-1)$-particle cluster due to the incident field and the field scattered by the Nth particle. This field is expressed as

$$\begin{aligned} \mathbf{E}_{N-1,\mathrm{cl}}^{(j)}(\mathbf{r}) &= \mathcal{R}g\{\boldsymbol{\mathcal{E}}^{\mathrm{t}}(\mathbf{r}_j)\} \cdot (\boldsymbol{\beta}^{(j,0)} \cdot \mathbf{a} + \boldsymbol{\alpha}^{(j,N)} \cdot \mathbf{T}_N^{(N)} \cdot \boldsymbol{\beta}^{(N,0)} \cdot \mathbf{a}) \\ &\equiv \mathcal{R}g\{\boldsymbol{\mathcal{E}}^{\mathrm{t}}(\mathbf{r}_j)\} \cdot \mathbf{e}_{N-1,\mathrm{cl}}^{(j)}. \end{aligned} \tag{19}$$

The scattered field coefficients $\mathbf{f}^{(j)}$ in the N-particle system are then obtainable in terms of the known $\mathbf{T}_{N-1}^{(j)}$ matrix, and the cluster excitation field

$$\mathbf{f}_N^{(j)} = \mathbf{T}_{N-1}^{(j)} \cdot \mathbf{e}_{N-1,\mathrm{cl}}^{(j)}. \tag{20}$$

Inserting the results for $\mathbf{e}^{(j)}_{N-1,\mathrm{cl}}$ from equation (19) into equation (20) and using the definition for $\mathbf{T}^{(j)}_N$ (equation (14)) yield

$$\mathbf{T}^{(j)}_N = \mathbf{T}^{(j)}_{N-1} \cdot (\mathbf{I} + \boldsymbol{\alpha}^{(j,N)} \cdot \mathbf{T}^{(N)}_N \cdot \boldsymbol{\beta}^{(N,j)}). \tag{21}$$

The two coupled equations (18) and (21) can be solved by substituting equation (18) into equation (21), and performing a matrix inversion:

$$\mathbf{T}^{(N)}_N = \left(\mathbf{I} - \mathbf{T}^{(N)}_1 \cdot \sum_{k=1}^{N-1} \boldsymbol{\alpha}^{(N,k)} \cdot \mathbf{T}^{(k)}_{N-1} \cdot \boldsymbol{\alpha}^{(k,N)}\right)^{-1} \cdot \mathbf{T}^{(N)}_1 \cdot \left(\mathbf{I} + \sum_{j=1}^{N-1} \boldsymbol{\alpha}^{(N,j)} \cdot \mathbf{T}^{(j)}_{N-1} \cdot \boldsymbol{\beta}^{(j,N)}\right). \tag{22}$$

Unlike the matrix inversion in equation (10), this inversion is performed on a basis set describing a single scatterer, and not the entire system. Once $\mathbf{T}^{(N)}_N$ has been determined, $\mathbf{T}^{(j)}_N$ may be determined by inserting $\mathbf{T}^{(N)}_N$ in equation (21). Equations (22) and (21) thus form a recursive algorithm by which all $\mathbf{T}^{(j)}_N$ matrices can be obtained for an arbitrary N-particle system.

For a two-particle system, $\mathbf{T}^{(j)}_2$ may be written symmetrically:

$$\mathbf{T}^{(1)}_2 = (\mathbf{I} - \mathbf{T}^{(1)}_1 \cdot \boldsymbol{\alpha}^{(1,2)} \cdot \mathbf{T}^{(2)}_1 \cdot \boldsymbol{\alpha}^{(2,1)})^{-1} \cdot \mathbf{T}^{(1)}_1 \cdot (\mathbf{I} + \boldsymbol{\alpha}^{(1,2)} \cdot \mathbf{T}^{(2)}_1 \cdot \boldsymbol{\beta}^{(2,1)}), \tag{23a}$$

$$\mathbf{T}^{(2)}_2 = (\mathbf{I} - \mathbf{T}^{(2)}_1 \cdot \boldsymbol{\alpha}^{(2,1)} \cdot \mathbf{T}^{(1)}_1 \cdot \boldsymbol{\alpha}^{(1,2)})^{-1} \cdot \mathbf{T}^{(2)}_1 \cdot (\mathbf{I} + \boldsymbol{\alpha}^{(2,1)} \cdot \mathbf{T}^{(1)}_1 \cdot \boldsymbol{\beta}^{(1,2)}). \tag{23b}$$

This result for a two-particle system is essentially that originally obtained by Bruning and Lo [12]. Simple manipulation of the geometric expansion formula for operators allows us to rewrite the above equations in a form which is more transparent for the developments of the next section:

$$\begin{aligned} \mathbf{T}^{(1)}_2 &= \mathbf{T}^{(1)}_1 \cdot (\mathbf{I} - \boldsymbol{\alpha}^{(1,2)} \cdot \mathbf{T}^{(2)}_1 \cdot \boldsymbol{\alpha}^{(2,1)} \cdot \mathbf{T}^{(1)}_1)^{-1} \cdot (\mathbf{I} + \boldsymbol{\alpha}^{(1,2)} \cdot \mathbf{T}^{(2)}_1 \cdot \boldsymbol{\beta}^{(2,1)}), \\ \mathbf{T}^{(2)}_2 &= \mathbf{T}^{(2)}_1 \cdot (\mathbf{I} - \boldsymbol{\alpha}^{(2,1)} \cdot \mathbf{T}^{(1)}_1 \cdot \boldsymbol{\alpha}^{(1,2)} \cdot \mathbf{T}^{(2)}_1)^{-1} \cdot (\mathbf{I} + \boldsymbol{\alpha}^{(2,1)} \cdot \mathbf{T}^{(1)}_1 \cdot \boldsymbol{\beta}^{(1,2)}). \end{aligned} \tag{24}$$

Although the recursive method is formally exact, we remarked that numerical inaccuracies appear during the application of this technique to truncated addition–translation matrices. These difficulties can rapidly become quite severe and limit the application of the recursive technique as was recently pointed out by Siqueira and Sarabandi [4], during the preparation of this work. Although the difficulties appear already in the application of the recursive prescription to a two-particle system, they are most evident in the application of recurrence from N to $N+1$ where $N \geqslant 2$. Our appraisal of the source of these problems is essentially the same as Siqueira and Sarabandi, and we only review it rapidly here.

In the interest of concreteness, let us consider the application of the recursive algorithm of equations (22) and (21) to the calculation of a three-particle system. The individual transfer matrix $\mathbf{T}^{(3)}_3$ is then to be calculated from the formula

$$\mathbf{T}^{(3)}_3 = \left(\mathbf{I} - \mathbf{T}^{(3)}_1 \cdot \sum_{k=1}^{2} \boldsymbol{\alpha}^{(3,k)} \cdot \mathbf{T}^{(k)}_2 \cdot \boldsymbol{\alpha}^{(k,3)}\right)^{-1} \cdot \mathbf{T}^{(3)}_1 \cdot \left(\mathbf{I} + \sum_{j=1}^{2} \boldsymbol{\alpha}^{(3,j)} \cdot \mathbf{T}^{(j)}_2 \cdot \boldsymbol{\beta}^{(j,3)}\right). \tag{25}$$

Inserting the results for $\mathbf{T}^{(1)}_2$ and $\mathbf{T}^{(2)}_2$ given in equation (24), one readily observes that there are products of the form $\boldsymbol{\beta}^{(j,i)} \cdot \boldsymbol{\alpha}^{(i,3)}$ and $\boldsymbol{\beta}^{(j,i)} \cdot \boldsymbol{\beta}^{(i,3)}$. The problem with

dimensional cut-offs is now apparent. The multiplication of truncated translation–addition does not equal the truncation of the product, that is

$$\begin{aligned}[\boldsymbol{\beta}^{(j,i)}]_{LL} \cdot [\boldsymbol{\alpha}^{(i,3)}]_{LL} &\neq [\boldsymbol{\beta}^{(j,i)} \cdot \boldsymbol{\alpha}^{(i,3)}]_{LL},\\ [\boldsymbol{\beta}^{(j,i)}]_{LL} \cdot [\boldsymbol{\beta}^{(i,3)}]_{LL} &\neq [\boldsymbol{\beta}^{(j,i)} \cdot \boldsymbol{\beta}^{(i,3)}]_{LL}.\end{aligned} \tag{26}$$

One could in principle alleviate this problem by truncating at orders higher than the cut-off for individual spheres, but one finds that this higher order corresponds roughly to the Wiscombe [1] criteria applied to a circumscribing sphere encompassing the entire system. Such large dimensions are in practice cumbersome and diminish the practicality of the recursive technique.

We shall show in section 4.3, however, that all the partial wave dimensionality problems can be resolved by applying the recursive procedure to scatterer-centred transfer matrices.

4.3. *Recursive methods for scatterer-centred* **T** *matrices*

The dimensionality problems encountered in recursive constructions of the individual transfer matrices $\mathbf{T}_N^{(j)}$ can be brought under control by applying the recursive technique to the calculation of scatterer-centred transfer matrices $\mathbf{T}_N^{(j,k)}$. By comparison of their respective definitions in equations (13) and (14), we find that the $\mathbf{T}_N^{(j)}$ may be expressed in terms of the $\mathbf{T}_N^{(j,k)}$:

$$\mathbf{T}_N^{(j)} = \sum_{k=1}^{N} \mathbf{T}_N^{(j,k)} \cdot \boldsymbol{\beta}^{(k,j)}. \tag{27}$$

Using this relation, a simple inspection of the results for $\mathbf{T}_2^{(j)}$ in equation (24) permits us to deduce the following expressions for $\mathbf{T}_2^{(i,j)}$:

$$\begin{aligned}\mathbf{T}_2^{(1,1)} &= \mathbf{T}_1^{(1)} \cdot (\mathbf{I} - \boldsymbol{\alpha}^{(1,2)} \cdot \mathbf{T}_1^{(2)} \cdot \boldsymbol{\alpha}^{(2,1)} \cdot \mathbf{T}_1^{(1)}]^{-1}\\ &= \mathbf{T}_1^{(1)} + \mathbf{T}_1^{(1)} \cdot \boldsymbol{\alpha}^{(1,2)} \cdot \mathbf{T}_1^{(2)} \cdot (\mathbf{I} - \boldsymbol{\alpha}^{(2,1)} \cdot \mathbf{T}_1^{(1)} \cdot \boldsymbol{\alpha}^{(1,2)} \cdot \mathbf{T}_1^{(2)})^{-1} \cdot \boldsymbol{\alpha}^{(2,1)} \cdot \mathbf{T}_1^{(1)},\\ \mathbf{T}_2^{(1,2)} &= \mathbf{T}_1^{(1)}(\mathbf{I} - \boldsymbol{\alpha}^{(1,2)} \cdot \mathbf{T}_1^{(2)} \cdot \boldsymbol{\alpha}^{(2,1)} \cdot \mathbf{T}_1^{(1)})^{-1} \cdot \boldsymbol{\alpha}^{(1,2)} \cdot \mathbf{T}_1^{(2)},\\ \mathbf{T}_2^{(2,2)} &= \mathbf{T}_1^{(2)}(\mathbf{I} - \boldsymbol{\alpha}^{(2,1)} \cdot \mathbf{T}_1^{(1)} \cdot \boldsymbol{\alpha}^{(1,2)} \cdot \mathbf{T}_1^{(2)})^{-1},\\ \mathbf{T}_2^{(2,1)} &= \mathbf{T}_1^{(2)}(\mathbf{I} - \boldsymbol{\alpha}^{(2,1)} \cdot \mathbf{T}_1^{(1)} \cdot \boldsymbol{\alpha}^{(1,2)} \cdot \mathbf{T}_1^{(2)})^{-1} \cdot \boldsymbol{\alpha}^{(2,1)} \cdot \mathbf{T}_1^{(1)}.\end{aligned} \tag{28}$$

An important property of these scatterer-centred transfer matrices $\mathbf{T}_2^{(j,i)}$ is that they begin on the left with an ordinary one-particle transfer matrix of the type $\mathbf{T}_1^{(j)}$ and end on the right with a transfer matrix of the type $\mathbf{T}_1^{(i)}$. Since the one-body transfer matrices have a natural cut-off arising from the finite particle size, the $\mathbf{T}_2^{(j,i)}$ will generally have their dimension limited to those physically excited in the individual particles. We shall see below that this property continues to hold true when we go to $N > 2$ particle systems.

We can now obtain the transfer matrices for the three-body system by inserting the definition of the scatterer-centred $\mathbf{T}_2^{(j,i)}$ matrices of the two-body system (equation (28)) into the recursion relations of equation (22). We obtain then

$$\mathbf{T}_3^{(3)} = \mathbf{T}_1^{(3)} \cdot \left(\mathbf{I} - \sum_{j,k=1}^{2} \boldsymbol{\alpha}^{(3,k)} \cdot \mathbf{T}_2^{(k,j)} \cdot \boldsymbol{\beta}^{(j,k)} \cdot \boldsymbol{\alpha}^{(k,3)} \cdot \mathbf{T}_1^{(3)} \right)^{-1}$$

$$\cdot \left(\mathbf{I} + \sum_{j,k=1}^{2} \boldsymbol{\alpha}^{(3,j)} \cdot \mathbf{T}_2^{(j,k)} \cdot \boldsymbol{\beta}^{(k,j)} \cdot \boldsymbol{\beta}^{(j,3)} \right). \tag{29}$$

We now see the advantage of the scatterer-centred formalism in which the regular translation matrices are kept explicitly outside of the $\mathbf{T}_N^{(j,k)}$ transfer matrices. The multiplications of the translation matrices in equation (29) may now be carried out formally to finite order by making use of the infinite-order addition matrix relations

$$\begin{aligned} \boldsymbol{\beta}^{(j,k)} \cdot \boldsymbol{\alpha}^{(k,3)} &= \boldsymbol{\alpha}^{(j,3)}, \\ \boldsymbol{\beta}^{(k,j)} \cdot \boldsymbol{\beta}^{(j,3)} &= \boldsymbol{\beta}^{(k,3)}. \end{aligned} \tag{30}$$

Consequently, equation (29) may be compactly rewritten

$$\mathbf{T}_3^{(3)} = \mathbf{T}_1^{(3)} \cdot \left(\mathbf{I} - \sum_{j,k=1}^{2} \boldsymbol{\alpha}^{(3,k)} \cdot \mathbf{T}_2^{(k,j)} \cdot \boldsymbol{\alpha}^{(j,3)} \cdot \mathbf{T}_1^{(3)} \right)^{-1} \left(\mathbf{I} + \sum_{j,k=1}^{2} \boldsymbol{\alpha}^{(3,j)} \cdot \mathbf{T}_2^{(j,k)} \cdot \boldsymbol{\beta}^{(k,3)} \right). \tag{31}$$

Carrying out the same procedure for an arbitrary N-particle system yields the recursive equation

$$\mathbf{T}_N^{(N)} = \mathbf{T}_1^{(N)} \cdot 1 \left(\mathbf{I} - \sum_{j,k=1}^{N-1} \boldsymbol{\alpha}^{(N,k)} \cdot \mathbf{T}_{N-1}^{(k,j)} \cdot \boldsymbol{\alpha}^{(j,N)} \cdot \mathbf{T}_1^{(N)} \right)^{-1} \cdot \left(\mathbf{I} + \sum_{j,k=1}^{N-1} \boldsymbol{\alpha}^{(N,j)} \cdot \mathbf{T}_{N-1}^{(j,k)} \cdot \boldsymbol{\beta}^{(k,N)} \right)$$

$$\equiv \sum_{k=1}^{N} \mathbf{T}_N^{(N,k)} \cdot \boldsymbol{\beta}^{(k,N)}. \tag{32}$$

As in the two-particle case, the identification of the $\mathbf{T}_N^{(N,k)}$ matrices is made by inspection, and the criteria that $\mathbf{T}_N^{(N,k)}$ begin with a matrix $\mathbf{T}_1^{(N)}$ and end with a matrix $\mathbf{T}_1^{(k)}$. This prescription yields

$$\mathbf{T}_N^{(N,N)} = \mathbf{T}_1^{(N)} \cdot \left(\mathbf{I} - \sum_{j,k=1}^{N-1} \boldsymbol{\alpha}^{(N,k)} \cdot \mathbf{T}_{N-1}^{(k,j)} \cdot \boldsymbol{\alpha}^{(j,N)} \cdot \mathbf{T}_1^{(N)} \right)^{-1}, \tag{33 a}$$

$$\mathbf{T}_N^{(N,k)} = \mathbf{T}_N^{(N,N)} \cdot \sum_{j=1}^{N-1} \boldsymbol{\alpha}^{(N,j)} \cdot \mathbf{T}_{N-1}^{(j,k)}, \qquad k \neq N. \tag{33 b}$$

The readjustment of the $\mathbf{T}_{N-1}^{(j,k)}$ matrices, $j \neq N$, $k \neq N$, so that they become N-body scatterer-centred matrices $\mathbf{T}_N^{(j,k)}$ is obtained by inserting equations (27) and (33 *a*) into the recursive equation (21), yielding

$$\begin{aligned}\mathbf{T}_N^{(j)} &= \sum_{i=1}^{N-1} \mathbf{T}_{N-1}^{(j,i)} \cdot \boldsymbol{\beta}^{(i,j)} \cdot \left(\mathbf{I} + \boldsymbol{\alpha}^{(j,N)} \cdot \sum_{k=1}^{N} \mathbf{T}_N^{(N,k)} \cdot \boldsymbol{\beta}^{(k,j)} \right) \\ &= \sum_{k=1}^{N-1} \left(\mathbf{T}_{N-1}^{(j,k)} + \sum_{i=1}^{N-1} \mathbf{T}_{N-1}^{(j,i)} \cdot \boldsymbol{\alpha}^{(i,N)} \cdot \mathbf{T}_N^{(N,k)} \right) \cdot \boldsymbol{\beta}^{(k,j)} \\ &\quad + \sum_{i=1}^{N-1} \mathbf{T}_{N-1}^{(j,i)} \cdot \boldsymbol{\alpha}^{(i,N)} \cdot \mathbf{T}_N^{(N,N)} \cdot \boldsymbol{\beta}^{(N,j)} \\ &= \sum_{k=1}^{N} \mathbf{T}_N^{(j,k)} \cdot \boldsymbol{\beta}^{(k,j)}, \end{aligned} \tag{34}$$

where $\mathbf{T}_N^{(j,k)}$ is obtained once again by inspection as

$$\mathbf{T}_N^{(j,N)} = \sum_{k=1}^{N-1} \mathbf{T}_{N-1}^{(j,k)} \cdot \boldsymbol{\alpha}^{(k,N)} \cdot \mathbf{T}_N^{(N,N)}, \qquad j \neq N, \tag{35a}$$

$$\mathbf{T}_N^{(j,k)} = \mathbf{T}_{N-1}^{(j,k)} + \sum_{i=1}^{N-1} \mathbf{T}_{N-1}^{(j,i)} \cdot \boldsymbol{\alpha}^{(i,N)} \cdot \mathbf{T}_N^{(N,k)}, \qquad j,k \neq N. \tag{35b}$$

The set of four equations given in equations (33) and (35) yield a complete recursive system for finding the $\mathbf{T}_N^{(j,k)}$ matrices. We remark that, upon adding a particle, a single matrix inversion in a one-particle space is performed in equation (33 *a*). The other three equations involve only matrix multiplications.

5. Formulae for physical quantities

The scatterer-centred transfer matrices $\mathbf{T}_N^{(j,k)}$ contain all the information concerning the complete field configuration for any incident wave. This very detailed information needs, however, to be transformed to experimentally relevant quantities. In the interest of completeness when using our conventions, we review the formulae for fixed-orientation and notation-averaged cross-sections. For the derivations of these formulae, we refer the reader to [2], [5] and [13].

5.1. *Fixed-orientation and orientation-averaged scattering cross-sections*

An incident wave of particular interest for cross-sections is the homogeneous plane wave, $\mathbf{E}_{\mathrm{i}}^{\mathrm{plane}}$, described via a real wave-vector $\mathbf{k}$ and a (possibly complex) transverse polarization vector $\hat{\mathbf{e}}_\gamma$. The vector space of transverse polarizations is two dimensional, and we consider a basis of two orthogonal transverse polarizations distinguished by an index ($\gamma = 1, 2$). The coefficient vector for this special incident field is denoted by $\mathbf{p}_\gamma$:

$$\begin{aligned}\mathbf{E}_{\mathrm{i}}^{\mathrm{plane}}(\mathbf{r}) &= E \exp(\mathrm{i}\mathbf{k}\cdot\mathbf{r})\hat{\mathbf{e}}_\gamma \\ &\equiv E\mathcal{R}g\{\boldsymbol{\mathcal{E}}^{\mathrm{t}}(k\mathbf{r})\} \cdot \mathbf{p}_\gamma. \end{aligned} \tag{36}$$

The plane-wave coefficients can be compactly expressed as ordinary (three) vector scalar products between $\hat{\mathbf{e}}_\gamma$ and the transverse vector spherical harmonics (see appendix A):

$$[\mathbf{p}_\gamma]^{\mathbf{M}}_{nm} = -\mathrm{i}^n 4\pi \mathbf{X}^*_{nm}(\hat{\mathbf{k}})\cdot\hat{\mathbf{e}}_\gamma, \quad (\mathbf{p}_\gamma)^{\mathbf{N}}_{nm} = -\mathrm{i}^{n+1} 4\pi \mathbf{Z}^*_{nm}(\hat{\mathbf{k}})\cdot\hat{\mathbf{e}}_\gamma. \tag{37}$$

As we shall see below, cross-sections will commonly take the form of $\mathbf{p}^\dagger_\gamma \cdot \mathbf{A} \cdot \mathbf{p}_\gamma$. The matrix $\mathbf{A}$ will generally contain regular translation matrices which act on $\mathbf{p}_\gamma$ and $\mathbf{p}^\dagger_\gamma$. Since the $\mathbf{p}_\gamma$ contain non-negligible components up to infinite order, this is potentially the source of new truncation problems. Fortunately, the particularly simple translation properties of incident plane waves result in the fact that their spherical coefficient vectors $\mathbf{p}_\gamma$ are eigenvectors of the regular translation matrices [13], that is

$$\begin{aligned} \boldsymbol{\beta}(k\mathbf{x})\cdot\mathbf{p}_\gamma &= \exp(\mathrm{i}\mathbf{k}\cdot\mathbf{x})\mathbf{p}_\gamma, \\ \mathbf{p}^\dagger_\gamma\cdot\boldsymbol{\beta}^\dagger(k\mathbf{x}) &= \exp(-\mathrm{i}\mathbf{k}\cdot\mathbf{x})\mathbf{p}^\dagger_\gamma. \end{aligned} \tag{38}$$

This 'phase' procedure then alleviates truncation problems associated with the regular translation–addition matrices [13]. We shall see below that equations (38) will readily allow the evaluation of all the cross-section formulae presented below.

For orientation-averaged cross-sections, one follows the trace techniques elaborated by Mackowski [5]. Using angular brackets $\langle\ \rangle_{\mathrm{o}}$ to denote the orientation average, one remarks that an orientation average of the matrix $\mathbf{A}$ corresponds to averaging the incident wave over all possible angles and polarizations, that is

$$\langle\mathbf{A}\rangle_{\mathrm{o}} \equiv \mathbf{p}^\dagger_\gamma\cdot\langle\mathbf{A}\rangle_{\mathrm{o}}\cdot\mathbf{p}_\gamma = \frac{1}{2}\frac{1}{4\pi}\sum_{\gamma=1}^{2}\int \mathrm{d}\Omega_{\mathbf{k}}\ [\mathbf{p}^\dagger_\gamma]\cdot\mathbf{A}\cdot[\mathbf{p}_\gamma]. \tag{39}$$

From equation (37) and the angular integrals for the normalized vector spherical harmonics (equation (A 3)), it follows immediately that

$$\int \mathrm{d}\Omega_{\mathbf{k}}\ [\mathbf{p}^\dagger_\gamma]^{\mathbf{A}}_{\nu\mu}[\mathbf{p}_\delta]^{\mathbf{B}}_{nm} = 16\pi^2\delta_{\mathbf{A},\mathbf{B}}\delta_{n,\nu}\delta_{m,\mu}\delta_{\gamma,\delta}, \tag{40}$$

from which one obtains

$$\langle\mathbf{A}\rangle_{\mathrm{o}} = 2\pi\,\mathrm{Tr}\,(\mathbf{A}). \tag{41}$$

We shall see below, for the quantities treated here, that the trace can be limited to the dimensional cut-off appropriate to the Mie scattering matrices.

Two of the quantities of interest are the extinction and scattering cross-sections of a cluster of N spheres ($\sigma^{\mathrm{cl}}_{\mathrm{e}}$ and $\sigma^{\mathrm{cl}}_{\mathrm{s}}$ respectively). It turns out to be convenient to write them as the sum of individual 'cross-sections' $\sigma^{(j)}_{\mathrm{e}}$ and $\sigma^{(j)}_{\mathrm{s}}$:

$$\sigma^{\mathrm{cl}}_{\mathrm{e}} = \sum_j^N \sigma^{(j)}_{\mathrm{e}}, \qquad \sigma^{\mathrm{cl}}_{\mathrm{s}} = \sum_j^N \sigma^{(j)}_{\mathrm{s}}. \tag{42}$$

It is important to remark that, although these individual 'cross-sections' can contain interesting physical information, they should not be considered as true cross-sections in the sense that they are defined using only part of the total field. Consequently, $\sigma^{(j)}_{\mathrm{e}}$ and $\sigma^{(j)}_{\mathrm{s}}$ do not necessarily satisfy relations typical of true cross-sections (positivity and individual energy conservation) [13]. The cluster cross-sections $\sigma^{\mathrm{cl}}_{\mathrm{e}}$ and $\sigma^{\mathrm{cl}}_{\mathrm{s}}$ on the other hand are physical cross-sections.

The individual extinction 'cross-sections' for a given incident plane wave can be written

$$\sigma_{\mathrm{e}}^{(j)}(\theta_{\mathrm{i}},\phi_{\mathrm{i}}) = -\frac{1}{k^2}\sum_{k}\mathrm{Re}\,(\mathbf{p}^{\dagger}\cdot\boldsymbol{\beta}^{(0,j)}\cdot\mathbf{T}_N^{(j,k)}\cdot\boldsymbol{\beta}^{(k,0)}\cdot\mathbf{p})$$

$$= -\frac{1}{k^2}\sum_{k}\mathrm{Re}\,\{\exp\,[\mathrm{i}\mathbf{k}\cdot(\mathbf{x}_k-\mathbf{x}_j)]\mathbf{p}^{\dagger}\cdot\mathbf{T}_N^{(j,k)}\cdot\mathbf{p}\}. \tag{43}$$

In the second line, the phase shift formulae of equation (38) have been invoked. The orientation average of the extinction cross-section is obtained by applying equation (41):

$$\langle\sigma_{\mathrm{e}}^{(j)}\rangle_{\mathrm{o}} = -\frac{2\pi}{k^2}\sum_{k}\mathrm{Re}\,[\mathrm{Tr}\,(\mathbf{T}_N^{(j,k)}\cdot\boldsymbol{\beta}^{(k,j)})], \tag{44}$$

where we have invoked the permutation properties of the trace. From the truncation properties of $\mathbf{T}_N^{(j,k)}$, discussed in section 4.3, it is now clear that the trace in this equation can in most cases be reliably restricted to the dimensions of the appropriate Mie transfer matrices.

The individual scattering 'cross-sections' can be written

$$\sigma_{\mathrm{s}}^{(j)}(\theta_{\mathrm{i}},\phi_{\mathrm{i}}) = \frac{1}{k^2}\mathrm{Re}\left(\sum_{l=1}^{N}\mathbf{f}^{(j)\dagger}\cdot\boldsymbol{\beta}^{(j,l)}\cdot\mathbf{f}^{(l)}\right), \tag{45}$$

where $\mathbf{f}^{(j)}$ are the scattering vectors given by

$$\mathbf{f}^{(j)} = \sum_{k=1}^{N}\mathbf{T}_N^{(j,k)}\cdot\boldsymbol{\beta}^{(k,0)}\cdot\mathbf{p} = \sum_{k=1}^{N}\exp\,(\mathrm{i}\mathbf{k}\cdot\mathbf{x}_k)\mathbf{T}_N^{(j,k)}\cdot\mathbf{p}. \tag{46}$$

An application of equation (41) and the permutation under the trace yield the orientation-averaged scattering cross-section.

$$\langle\sigma_{\mathrm{s}}^{(j)}\rangle_{\mathrm{o}} = \frac{2\pi}{k^2}\mathrm{Re}\left(\sum_{k,l,l}^{N}\mathrm{Tr}\,([\mathbf{T}_N^{(j,l)}]^{\dagger}\cdot\boldsymbol{\beta}^{(\mathrm{j},k)}\cdot\mathbf{T}_N^{(k,i)}\cdot\boldsymbol{\beta}^{(i,l)}\right). \tag{47}$$

Although the cluster absorption cross-section $\sigma_{\mathrm{a}}^{\mathrm{cl}}$ in a non-absorbing media can be deduced from energy conservation, that is $\sigma_{\mathrm{a}}^{\mathrm{cl}} = \sigma_{\mathrm{e}}^{\mathrm{cl}} - \sigma_{\mathrm{s}}^{\mathrm{cl}}$, it may alternatively be calculated by evaluating the Poynting vector of the total field at the surface of the individual particles. Since the total field is used in their definition, the $\sigma_{\mathrm{a}}^{(j)}$ correspond to true physical cross-sections and are interpreted as the energy absorbed within the jth scatterer. Their sum is the absorption cross-section for the cluster: $\sigma_{\mathrm{a}}^{\mathrm{cl}} = \sum_{j}^{N}\sigma_{\mathrm{a}}^{(j)}$. The $\sigma_{\mathrm{a}}^{(j)}$ can be expressed as [13]

$$\sigma_{\mathrm{a}}^{(j)}(\theta_{\mathrm{i}},\phi_{\mathrm{i}}) = \frac{1}{k^2}\mathbf{f}^{(j)\dagger}\cdot\boldsymbol{\Gamma}^{(j)}\cdot\mathbf{f}_{\mathrm{s}}^{(j)},$$

$$\langle\sigma_{\mathrm{a}}^{(j)}\rangle_{\mathrm{o}} = \frac{2\pi}{k^2}\sum_{k,l}\mathrm{Tr}\,([\mathbf{T}_N^{(\mathrm{j},k)}]^{\dagger}\cdot\boldsymbol{\Gamma}^{(j)}\cdot\mathbf{T}_N^{(j,l)}\cdot\boldsymbol{\beta}^{(l,k)}), \tag{48}$$

where the absorption matrix $\boldsymbol{\Gamma}^{(j)}$ is of the form

$$\boldsymbol{\Gamma}^{(j)} = \begin{bmatrix}\mathbf{C}^{(j)} & \mathbf{0}\\ \mathbf{0} & \mathbf{D}^{(j)}\end{bmatrix}. \tag{49}$$

The $\mathbf{C}^{(j)}$ and $\mathbf{D}^{(j)}$ are diagonal matrices whose matrix elements are given by $[\mathbf{C}^{(j)}]_{nm,\nu\mu} = \delta_{n\nu}\delta_{m\mu}\mathbf{C}_n^{(j)}$, $[\mathbf{D}^{(j)}]_{nm,\nu\mu} = \delta_{n\nu}\delta_{m\mu}\mathbf{D}_n^{(j)}$, with

$$\mathbf{C}_n^{(j)} = \frac{\mathrm{Re}\left[\mathrm{i}\rho_j \mu \mu_j^* \psi_n^*(\rho_j\chi_j)\psi_n'(\rho_j\chi_j)\right]}{\left|\mu_j \psi_n(\rho_j\chi_j)\psi_n'(\chi_j) - \mu\rho_j\psi_n'(\rho_j\chi_j)\psi_n(\chi_j)\right|^2},$$
$$\mathbf{D}_n^{(j)} = \frac{\mathrm{Re}\left[\mathrm{i}\rho_j^* \mu \mu_j \psi_n^*(\rho_j\chi_j)\psi_n'(\rho_j\chi_j)\right]}{\left|\mu\rho_j \psi_n(\rho_j\chi_j)\psi_n'(\chi_j) - \mu_j\psi_n(\chi_j)\psi_n'(\rho_j\chi_j)\right|^2}, \tag{50}$$

where the functions $\psi_n(x)$ are Ricatti spherical Bessel functions: $\psi_n(x) \equiv x j_n(x)$. In the particular case $\mu_j = \mu = 1$, this result reduces to the absorption formula for spherical scatterers derived by Mackowski [2].

5.2. *Local field formulae*

The scatterer-centred transfer matrices not only are useful for far-field quantities such as the scattering cross-sections but also contain all the local field information as well. The field in the interior of the particle is a region of considerable interest. The electric field $\mathbf{E}_{\mathrm{I}}^{(j)}(\mathbf{r})$ in the interior of a particle j in an N-particle cluster is described via the internal field coefficients $\mathbf{i}^{(j)}$:

$$\mathbf{E}_{\mathrm{I}}^{(j)}(\mathbf{r}) \equiv \mathcal{R}g\left\{\boldsymbol{\mathcal{E}}^t(k\mathbf{r}_j)\right\} \cdot \mathbf{i}^{(j)}. \tag{51}$$

For spherical particles, these coefficients are given by [8, 9]

$$\begin{aligned}\mathbf{i}^{(j)} &= \boldsymbol{\Lambda}^{(j)} \cdot \mathbf{f}^{(j)} \\ &= \sum_{k=1}^{N} \boldsymbol{\Lambda}^{(j)} \cdot \mathbf{T}_N^{(j,k)} \cdot \boldsymbol{\beta}^{(k,0)} \cdot \mathbf{a},\end{aligned} \tag{52}$$

where $\boldsymbol{\Lambda}^{(j)}$ is a diagonal matrix given by

$$\boldsymbol{\Lambda}^{(j)} = \begin{bmatrix} \boldsymbol{\Lambda}^{\mathbf{M},(j)} & \mathbf{0} \\ \mathbf{0} & \boldsymbol{\Lambda}^{\mathbf{N},(j)} \end{bmatrix} \tag{53}$$

with

$$\boldsymbol{\Lambda}^{\mathbf{M},(j)}_{nm,\nu\mu} = \delta_{n\nu}\delta_{m\mu} \frac{\mathrm{i}\mu_j\rho_j}{\mu\rho_j\psi_n'(\rho_j\chi_j)\psi_n(\chi_j) - \mu_j\psi_n(\rho_j\chi_j)\psi_n'(\chi_j)},$$
$$\boldsymbol{\Lambda}^{\mathbf{N},(j)}_{nm,\nu\mu} = \delta_{n\nu}\delta_{m\mu} \frac{\mathrm{i}\mu_j\rho_j}{\mu_j\psi_n(\chi_j)\psi_n'(\rho_j\chi_j) - \mu\rho_j\psi_n(\rho_j\chi_j)\psi_n'(\chi_j)}.$$

The above formulae are generally sufficient for determining the interior field point by point.

If one is interested in angular or spatial averages of the squared electric field amplitude $|\mathbf{E}_{\mathrm{I}}^{(j)}(\mathbf{r}_j)|^2$ inside the scatterers, it is preferable to carry out the angular integrations analytically. The squared amplitude of the electric field in the interior of the scatterer can be expressed as

$$\begin{aligned}|\mathbf{E}_{\mathrm{I}}^{(j)}(\mathbf{r}_j)|^2 &= [\mathbf{f}^{(j)}]^\dagger \cdot [\boldsymbol{\Lambda}^{(j)}]^\dagger \cdot \boldsymbol{\mathcal{E}}^*(k\mathbf{r}_j) \cdot \boldsymbol{\mathcal{E}}^{\mathrm{t}}(k\mathbf{r}_j) \cdot \boldsymbol{\Lambda}^{(j)} \cdot \mathbf{f}^{(j)} \\ &= [\mathbf{f}^{(j)}]^\dagger \cdot [\boldsymbol{\Lambda}^{(j)}]^\dagger \cdot \boldsymbol{\Pi}(\mathbf{r}_j) \cdot \boldsymbol{\Lambda}^{(j)} \cdot \mathbf{f}^{(j)},\end{aligned} \tag{54}$$

where the $\boldsymbol{\Pi}(\mathbf{r}_j)$ matrix is defined as

$$\mathbf{\Pi}(\mathbf{r}_j) \equiv \boldsymbol{\mathcal{E}}^*(k\mathbf{r}_j)\cdot\boldsymbol{\mathcal{E}}^{\mathrm{t}}(k\mathbf{r}_j) = \begin{bmatrix} \mathbf{\Pi}^{\mathbf{MM}}(\mathbf{r}_j) & \mathbf{\Pi}^{\mathbf{MN}}(\mathbf{r}_j) \\ \mathbf{\Pi}^{\mathbf{NM}}(\mathbf{r}_j) & \mathbf{\Pi}^{\mathbf{NN}}(\mathbf{r}_j) \end{bmatrix}. \tag{55}$$

The components of this matrix are determined from the definitions of the spherical wave-vectors (equation (69)), yielding

$$\begin{aligned}
\mathit{\Pi}^{\mathbf{MM}}_{nm,\nu\mu}(\mathbf{r}) &= j_n^*(k_j r) j_\nu(k_j r)\mathbf{X}^*_{nm}(\hat{\mathbf{r}})\cdot\mathbf{X}_{\nu\mu}(\hat{\mathbf{r}}),\\
\mathit{\Pi}^{\mathbf{MN}}_{nm,\nu\mu}(\mathbf{r}) &= -j_n^*(k_j r)\frac{1}{k_j r}[k_j r j_\nu(k_j r)]'\mathbf{X}^*_{nm}(\hat{\mathbf{r}})\cdot\mathbf{Z}_{\nu\mu}(\hat{\mathbf{r}}),\\
\mathit{\Pi}^{\mathbf{NM}}_{nm,\nu\mu}(\mathbf{r}) &= -\frac{1}{k_j^* r}[k_j^* r j_n^*(k_j r)]' j_\nu(k_j r)\mathbf{Z}^*_{nm}(\hat{\mathbf{r}})\cdot\mathbf{X}_{\nu\mu}(\hat{\mathbf{r}}),\\
\mathit{\Pi}^{\mathbf{NN}}_{nm,\nu\mu}(\mathbf{r}) &= \frac{1}{|k_j r|^2}[n(n+1)]^{1/2}[\nu(\nu+1)]^{1/2} j_n^*(k_j r) j_\nu(k_j r)\mathbf{Y}^*_{nm}(\hat{\mathbf{r}})\cdot\mathbf{Y}_{\nu\mu}(\hat{\mathbf{r}})\\
&\quad + \frac{1}{|k_j r|^2}[k_j^* r j_n^*(k_j r)]'[k_j r j_\nu(k_j r)]'\mathbf{Z}^*_{nm}(\hat{\mathbf{r}})\cdot\mathbf{Z}_{\nu\mu}(\hat{\mathbf{r}}).
\end{aligned} \tag{56}$$

A special value of interest is the field at the centre of the spheres for which we can exploit the limit relations

$$\lim_{x\to 0}[j_n(x)] \approx \frac{x^n}{(2n+1)!!}, \quad \lim_{x\to 0}\{[x j_\nu(x)]'\} \approx \frac{(n+1)x^n}{(2n+1)!!}. \tag{57}$$

A consequence of these relations is that only $\mathit{\Pi}^{\mathbf{NN}}_{1m,1\mu}$ have a non-zero limit as $r \to 0$. Using

$$\mathit{\Pi}^{\mathbf{NN}}_{nm,\nu\mu}(r\to 0) = \delta_{n,1}\delta_{\nu,1}\tfrac{2}{9}\mathbf{Y}^*_{1m}(\hat{\mathbf{r}})\cdot\mathbf{Y}_{1\mu}(\hat{\mathbf{r}}) + \tfrac{4}{9}\delta_{n,1}\delta_{\nu,1}\mathbf{Z}^*_{1m}(\hat{\mathbf{r}})\cdot\mathbf{Z}_{1\mu}(\hat{\mathbf{r}}) \tag{58}$$

and the angular average integral

$$\frac{1}{4\pi}\int \mathrm{d}\Omega\, \mathit{\Pi}^{\mathbf{NN}}_{nm,\nu\mu}(r=0) = \frac{1}{6\pi}\delta_{n,1}\delta_{\nu,1}\delta_{m,\mu}, \tag{59}$$

we obtain that the field at the centre of the particles is

$$|\mathbf{E}_{\mathrm{I}}^{(j)}(\mathbf{0})|^2 = \frac{1}{6\pi}\sum_{m=-1}^{1}[[\mathbf{f}^{(j)}]^\dagger\cdot[\boldsymbol{\Lambda}^{(j)}]^\dagger]^{\mathbf{N}}_{1,m}[\boldsymbol{\Lambda}^{(j)}\cdot\mathbf{f}^{(j)}]^{\mathbf{N}}_{1,m}. \tag{60}$$

At a finite distance r from the particle centre, the angular average of $|\mathbf{E}_{\mathrm{I}}^{(j)}(\mathbf{r}_j)|^2$ is found from

$$\begin{aligned}
\int \mathrm{d}\Omega\, \mathit{\Pi}^{\mathbf{MM}}_{nm,\nu\mu}(\mathbf{r}) &= |j_n(k_j r)|^2\delta_{n,\nu}\delta_{m,\mu},\\
\int \mathrm{d}\Omega\, \mathit{\Pi}^{\mathbf{MN}}_{nm,\nu\mu}(\mathbf{r}) &= \int \mathrm{d}\Omega\, \mathit{\Pi}^{\mathbf{NM}}_{nm,\nu\mu} = 0,\\
\int \mathrm{d}\Omega\, \mathit{\Pi}^{\mathbf{NN}}_{nm,\nu\mu}(\mathbf{r}) &= n(n+1)\left|\frac{j_n(k_j r)}{k_j r}\right|^2\delta_{n,\nu}\delta_{m,\mu} + \left|\frac{[k_j^* r j_n^*(k_j r)]'}{k_j r}\right|^2\delta_{n,\nu}\delta_{m,\mu}.
\end{aligned} \tag{61}$$

The average $|\mathbf{E}_{\mathrm{I}}^{(j)}|^2_{\mathrm{avg}}$ of $|\mathbf{E}_{\mathrm{I}}^{(j)}(\mathbf{r}_j)|^2$ in the interior of the scatterers is then obtained via the integrals

$$\frac{1}{V_s}\int_{V_s} d^3r\, \Pi^{\mathbf{MM}}_{nm,\nu\mu}(\mathbf{r}) = \mathbf{I}_n\delta_{n,\nu}\delta_{m,\mu},$$
$$\frac{1}{V_s}\int_{V_s} d^3r\, \Pi^{\mathbf{MN}}_{nm,\nu\mu}(\mathbf{r}) = \int_0^R d^3r\, \Pi^{\mathbf{NM}}_{nm,\nu\mu} = 0, \tag{62}$$
$$\frac{1}{V_s}\int_{V_s} d^3r\, \Pi^{\mathbf{NN}}_{nm,\nu\mu}(\mathbf{r}) = \mathrm{J}_n\delta_{n,\nu}\delta_{m,\mu}.$$

The resulting expression for the average electric field intensity within the scatterers is

$$|\mathbf{E}_{\mathrm{I}}^{(j)}|^2_{\mathrm{avg}} = [\mathbf{f}^{(j)}]^\dagger \cdot [\mathbf{\Lambda}^{(j)}]^\dagger \cdot \begin{bmatrix} \mathbf{I} & \mathbf{0} \\ \mathbf{0} & \mathbf{J} \end{bmatrix} \cdot \mathbf{\Lambda}^{(j)} \cdot \mathbf{f}^{(j)}, \tag{63}$$

where the $\mathbf{I}$ and $\mathbf{J}$ matrices are diagonal (i.e. of the form $\mathrm{O}_{\nu\mu,nm} = \delta_{n,\nu}\delta_{m,\mu}\mathrm{O}_n$), with

$$\mathbf{I}_n = \frac{1}{V_s}\int_0^{R_j} dr\, r^2 |j_n(k_j r)|^2,$$
$$\mathbf{J}_n = \frac{1}{V_s}\left(\frac{n(n+1)}{|k_j|^2}\int_0^{R_j} dr\, |j_n(k_j r)|^2 + \frac{1}{|k_j|^2}\int_0^{R_j} dr\, |[k_j^* r j_n^*(k_j r)]'|^2\right). \tag{64}$$

Although these integrals can be carried out analytically for real k_j, they are best carried out numerically for complex k_j. We can also consider orientation averages of $|\mathbf{E}_{\mathrm{I}}^{(j)}(\mathbf{r}_j)|^2$. The orientation-averaged formula is once again obtained by applying equation (41):

$$\langle |\mathbf{E}_{\mathrm{I}}^{(j)}|^2_{\mathrm{avg}} \rangle_{\mathrm{o}} = 2\pi \sum_{l,k} \mathrm{Tr}\left([\mathbf{T}_N^{(j,l)}]^\dagger \cdot [\boldsymbol{\Lambda}^{(j)}]^\dagger \cdot \begin{bmatrix} \mathbf{I} & \mathbf{0} \\ \mathbf{0} & \mathbf{J} \end{bmatrix} \cdot \boldsymbol{\Lambda}^{(j)} \cdot \mathbf{T}_N^{(j,k)} \cdot \boldsymbol{\beta}^{(k,l)} \right). \tag{65}$$

6. Demonstrative calculations

We now demonstrate applications of the formulae elaborated in this work to the problem of fields inside the scatterers for conditions ranging from weak to strong scattering. In the interest of applications to a physical system, we consider systems of identical dielectric scatterers of refraction index $n_s \approx 2.5$ (approximately that of TiO_2) in a dielectric host medium of index $n \approx 1.5$ (corresponding to common polymers). Since there is no absorption in our theoretical system, the extinction and scattering cross-sections will be identical. We present below some illustrative calculations for scattering as a function of the size parameter χ of the individual spheres. The size parameter is $\chi \equiv kR = 2\pi r/\lambda$, where λ is the wavelength in the host media and R is the radius of the spheres.

In order to fix the ideas, let us consider first a system of two touching spheres. As we saw in previous sections, the $\mathbf{T}_2^{(j,k)}$ matrices allow us to calculate the local fields. Using equation (63), we show in figure 2 (*a*) the average squared internal electric fields $|\mathbf{E}_{\mathrm{I}}^{(1)}|^2_{\mathrm{avg}}/E^2$ and $|\mathbf{E}_{\mathrm{I}}^{(2)}|^2_{\mathrm{avg}}/E^2$ of the two-particle cluster for an incident plane wave arriving along the axis of symmetry of the two spheres. We divide by the squared field amplitude E^2 of the incident wave in order to plot dimensionless quantities. Sphere 1 is chosen to be the first sphere encountered along the direction

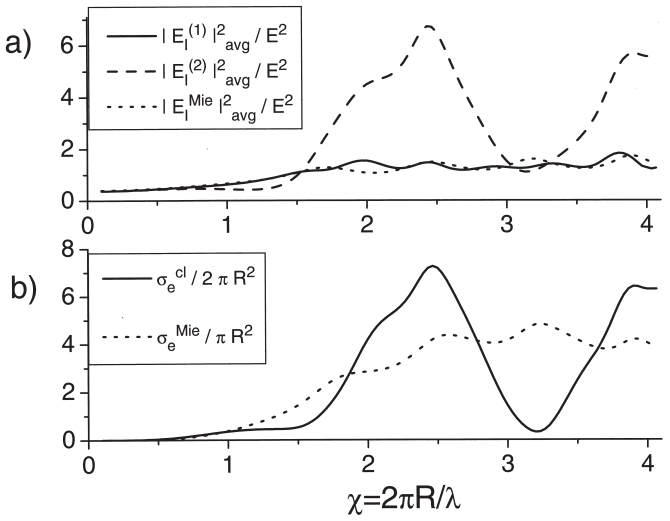

Figure 2. A two-particle system of two touching spheres, with $n_{sp} = 2.5$ and $n = 1.5$. The incident wave is oriented along the symmetry axis of the system. Sphere 1 is the sphere 'first' encountered by the incident beam. (*a*) A plot of the average squared internal electric field $|\mathbf{E}_I^{(j)}|^2_{avg}$, $j = 1, 2$, of each sphere and the average squared internal electric field $|\mathbf{E}_I^{Mie}|^2_{avg}$ of an independent Mie sphere. (*b*) A plot of the normalized cross-section $\sigma_e^{cl}/2\pi R^2$ per sphere of this system and the cross-section $\sigma_e^{Mie}/\pi R^2$ of an independent Mie sphere.

of propagation, **k**; sphere 2 is then the second sphere encountered. For the purpose of comparison, we also illustrate the average internal field for an isolated sphere. We remark that the average internal field in sphere 1 is quite similar to that of an isolated sphere, while the 'shadowed' sphere 2 is considerably modified from that of an isolated sphere.

In figure 2 (*b*), we use equation (43) to calculate the total normalized extinction (scattering) cross-section $\sigma_e^{cl}/2\pi R^2$ of the two-sphere system. By 'normalized', we mean that we divide σ_e^{cl} by the total geometric cross-section $2\pi R^2$ of the two-particle system (not taking into account overlap). For comparison with the independent scattering cross-section, we also show the normalized cross-section $\sigma_e^{Mie}/\pi R^2$ of an isolated (Mie) sphere. It is interesting to observe that peaks in internal field amplitudes in figure 2 (*a*) generally correspond to total cross-section peaks in figure 2 (*b*).

One might be tempted to conclude from figure 2 that dependent scattering can make large quantitative and qualitative corrections to independent scattering. We should keep in mind, however, that the quantities in figure 2 were calculated with a fixed orientation of the two-sphere system with respect to the incident plane wave. Moreover, the chosen configuration optimizes coherent field effects. In applications to random inhomogeneous media, however, one is generally more interested in orientation-averaged scattering rather than in the scattering produced by a particular configuration. We shall now show that the above qualitative corrections to independent scattering are largely washed out when one considers orientation-averaged quantities.

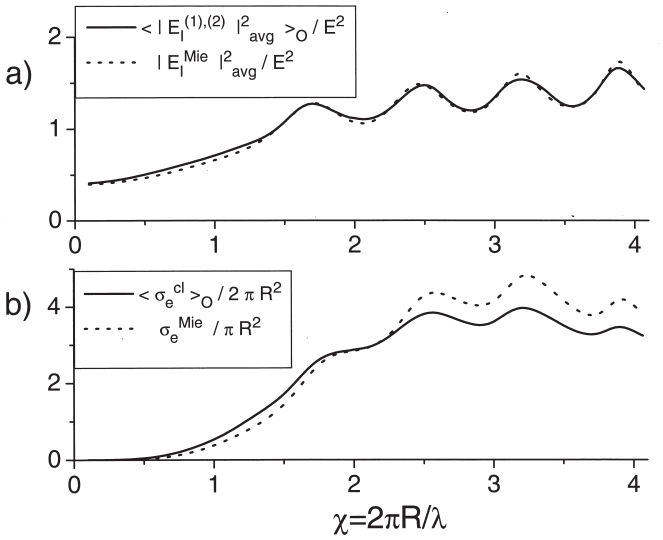

Figure 3. The same physical quantities for the two-sphere system studied in figure 2 after orientation averaging. (*a*) A plot of $\langle |\mathbf{E}_I^{(1)}|^2_{avg}\rangle_o = \langle |\mathbf{E}_I^{(2)}|^2_{avg}\rangle_o$ versus $|\mathbf{E}_I^{Mie}|^2_{avg}$. (*b*) Plot of the normalized orientation averaged cross-section $\langle \sigma_e^{cl}\rangle_o / 2\pi R^2$ per sphere, compared with the independent scattering cross-section $\sigma_e^{Mie}/\pi R^2$.

In figure 3 (*a*), we carry out configuration averages of the average squared internal fields $|\mathbf{E}_I^{(j)}|^2_{avg}/E^2$ using equation (65). After the configuration average, the fields in the two spheres are identical: $\langle |\mathbf{E}_I^{(1)}|^2_{avg}\rangle_o = \langle |\mathbf{E}_I^{(2)}|^2_{avg}\rangle_o$. Comparing these field averages with the field average $|\mathbf{E}_I^{Mie}|^2_{avg}$ of an isolated scatterer, we see that the difference is hardly distinguishable. In figure 3 (*b*), we compare the orientation-averaged cross-section $\langle \sigma_e^{cl}\rangle_o / 2\pi R^2$ with that for independent scattering, $\sigma_e^{Mie}/\pi R^2$. It is striking that, after orientation averaging, the two curves have the same qualitative behaviour, and that dependent scattering effects simply correspond to a slight lowering of the cross-section per sphere for $\chi \gtrsim 2$. We remark onced again that peaks in the orientation-averaged internal field generally correspond to peaks in the cross-section.

It is natural to ask at this point to what extent additional spheres will modify the above scenario. We thus look to obtain some response to this question by carrying out analogous calculations for a seven-particle system. In this system, we place on sphere centred at the origin of the coordinate system. We then place pairs of spheres on each of the $\hat{\mathbf{x}}$, $\hat{\mathbf{y}}$ and $\hat{\mathbf{z}}$ axes. Each of the six 'exterior' spheres is placed such that they touch the sphere at the origin. We call the sphere at the origin sphere 1. Spheres 2 and 3 are on the positive and negative $\hat{\mathbf{z}}$ axes respectively. Spheres 4 and 5 are on the $\hat{\mathbf{x}}$ axis, while spheres 6 and 7 are on the $\hat{\mathbf{y}}$ axis.

In figure 4 (*a*) we show the internal fields in these spheres as a function of the size parameter for an incident plane wave with a propagation vector oriented in the positive $\hat{\mathbf{z}}$ direction, and a linear polarization along the $\hat{\mathbf{y}}$ axis. Symmetry considerations tell us in advance that spheres 4 and 5 will have the same internal fields, as will also spheres 6 and 7 (confirmed by calculations). The pair 4 and 5 are not identical with the pair 6 and 7, however, on account of the fact that they have different orientations with respect to the incident field polarization. On the scale of

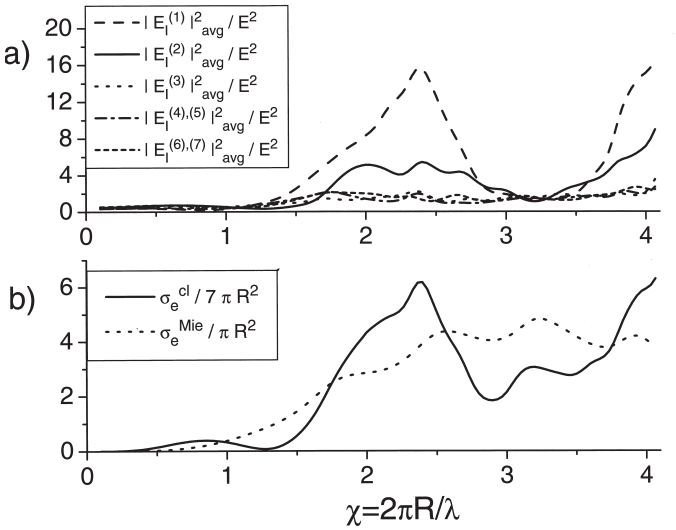

Figure 4. System of seven identical touching spheres with $n_{sp} = 2.5$ and $n = 1.5$. (*a*) A plot of the averaged squared internal electric field $|\mathbf{E}_I^{(j)}|^2_{avg}$, $j = 1, \ldots, 7$, of each sphere. (*b*) A plot of the normalized cross-section $\sigma_e^{cl}/7\pi R^2$ per sphere of this system and the cross-section $\sigma_e^{Mie}/\pi R^2$ independent Mie sphere.

this graph, only the average internal fields spheres in spheres 1 and 2 stand out significantly from the others. In figure 4 (*b*), we show the total cross-section per sphere and compare it with that of independent scatterers. As was the case with the two-particle system, there are considerable qualitative differences between the total cross-section per sphere and independent scattering.

After orientation averaging, all the spheres except for the central sphere will have identical average internal fields: $\langle|\mathbf{E}_I^{(2)}|^2_{avg}\rangle_o = \langle|\mathbf{E}_I^{(3)}|^2_{avg}\rangle_o = \cdots = \langle|\mathbf{E}_I^{(7)}|^2_{avg}\rangle_o$. The orientation averages $\langle|\mathbf{E}_I^{(j)}|^2_{avg}\rangle_o/E^2$ are plotted in figure 5 (*a*) and compared with those of independent scattering. We see that the average fields in spheres 2–7 are nearly indistinguishable from that of independent scattering, $|\mathbf{E}_I^{Mie}|^2_{avg}$. The average field in the central sphere 1 is slightly modified with respect to $|\mathbf{E}_I^{Mie}|^2_{avg}$ but has the same general behaviour. In figure 5 (*b*), we show the normalized orientation averaged cross-section $\langle\sigma_e^{cl}\rangle_o/7\pi R^2$ and compare it with the independent scattering cross-section. It is striking that the resonance peaks in the independent scattering are nearly completely washed out after the orientation average, and that the principle effect of dependent scattering is to increase slightly the per-sphere scattering cross-section for size parameter $\chi \lesssim 2$ and to quench it considerably for $\chi \gtrsim 2$. It is interesting to remark that, in the white-paint industry, size parameters of $\chi \approx 2$ are common.

7. Conclusions

The recursive techniques developed here permit numerically stable calculations of multiple-scattering systems. This technique is apparently free of convergence difficulties. Although it was not discussed in the text, the recursive equations are of a self-consistent nature, and any numerical errors arising from the large

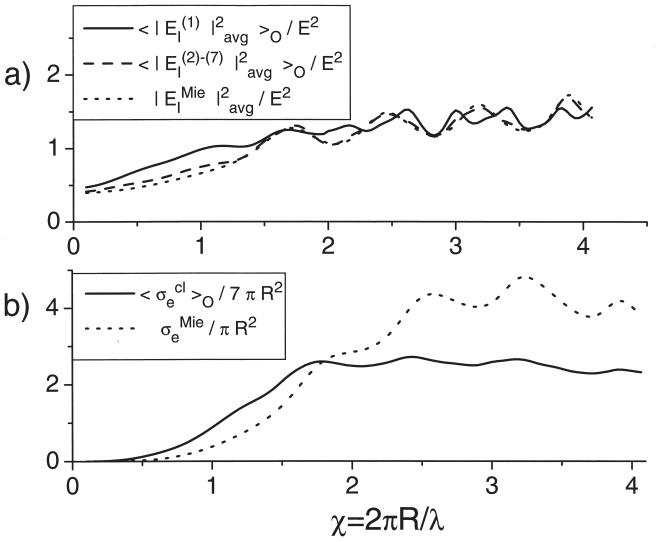

Figure 5. Orientation averages of the seven-sphere system. (*a*) A plot of $\langle \mathbf{E}_{\mathrm{I}}^{(1)}|^2_{\mathrm{avg}}\rangle_{\mathrm{o}}$ and $\langle \mathbf{E}_{\mathrm{I}}^{(2)}|^2_{\mathrm{avg}}\rangle_{\mathrm{o}} = \cdots = \langle |\mathbf{E}_{\mathrm{I}}^{(7)}|^2_{\mathrm{avg}}\rangle_{\mathrm{o}}$ versus that of an independent m:e sphere, $|\mathbf{E}_{\mathrm{I}}^{\mathrm{Mie}}|^2_{\mathrm{avg}}$. (*b*) A plot of the normalized orientation averaged cross-section $\langle \sigma_{\mathrm{e}}^{\mathrm{cl}}\rangle_{\mathrm{o}}/7\pi R^2$ per sphere compared with the independent scattering cross-section $\sigma_{\mathrm{e}}^{\mathrm{Mie}}/\pi R^2$.

number of calculations may be eliminated by employing this self-consistency at any stage of the calculations. One of the indications of the reliability of this technique is its ability to satisfy automatically any symmetries of the chosen multiple-scattering configuration. This is an important point since, as we add particles to the system, certain symmetries are only 'recovered' after a particular scatterer has been added.

We have demonstrated that the scatterer-centred transfer matrices $\mathbf{T}_N^{(i,j)}$ can give information on the local field within an aggregate as well as far-field cross-sections. The $\mathbf{T}_N^{(i,j)}$ are also particularly useful for obtaining analytic orientation averages. These analytic averages are more reliable than numerical averages and save considerable computational labour.

An interesting observation on the calculations in the last section is that, after orientation averaging, dependent scattering effects largely wash out the resonant field effects on the total cross-sections. Internal field densities inside the particles were only slightly modified, however. Total cross-sections are, however, a rather crude indication of the complete wave–particle interaction. It should prove interesting to study the dependent scattering effects on the angular distribution of the scattered wave after a configuration average. These effects will be studied in subsequent publications.

Acknowledgments

Brian Stout would like to thank Hervé Tortel and Sophie Stout for helpful discussions.

Appendix A. Spherical waves and vector spherical harmonics

The three normalized vector spherical harmonics used by us can be explicitly written in terms of the associated Legendre functions:

$$\begin{aligned}
\mathbf{Y}_{nm}(\hat{\mathbf{r}}) &= \gamma_{nm}[n(n+1)]^{1/2} P_n^m(\cos\theta)\exp(\mathrm{i}m\phi)\,\hat{\mathbf{r}} = Y_{nm}(\theta,\phi)\hat{\mathbf{r}},\\
\mathbf{X}_{nm}(\hat{\mathbf{r}}) &= \gamma_{nm}\left(-\frac{\mathrm{i}m}{\sin\theta}P_n^m(\cos\theta)\exp(\mathrm{i}m\phi)\,\hat{\boldsymbol{\theta}} + \frac{\mathrm{d}}{\mathrm{d}\theta}P_n^m(\cos\theta)\exp(\mathrm{i}m\phi)\hat{\boldsymbol{\phi}}\right)\\
&\equiv -\mathrm{i}\bar{u}_n^m(\cos\theta)\exp(\mathrm{i}m\phi)\,\hat{\boldsymbol{\theta}} + \bar{s}_n^m(\cos\theta)\exp(\mathrm{i}m\phi)\,\hat{\boldsymbol{\phi}}, \qquad \text{(A 1)}\\
\mathbf{Z}_{nm}(\hat{\mathbf{r}}) &= \gamma_{nm}\left(\frac{\mathrm{d}}{\mathrm{d}\theta}P_n^m(\cos\theta)\exp(\mathrm{i}m\phi)\,\hat{\boldsymbol{\theta}} + \frac{\mathrm{i}m}{\sin\theta}P_n^m(\cos\theta)\exp(\mathrm{i}m\phi)\,\hat{\boldsymbol{\phi}}\right)\\
&\equiv \bar{s}_n^m(\cos\theta)\exp(\mathrm{i}m\phi)\,\hat{\boldsymbol{\theta}} + \mathrm{i}\bar{u}^m n(\cos\theta)\exp(\mathrm{i}m\phi)\,\hat{\boldsymbol{\phi}},
\end{aligned}$$

where the normalization coefficients γ_{nm} are defined by

$$\gamma_{nm} \equiv \left(\frac{(2n+1)(n-m)!}{4\pi n(n+1)(n+m)!}\right)^{1/2}. \qquad \text{(A 2)}$$

The normalized vector spherical harmonics satisfy the orthonormality condition

$$\int \mathrm{d}\Omega_{\mathbf{k}}\,\mathbf{A}^*_{n'm'}(\hat{\mathbf{k}})\cdot\mathbf{B}_{nm}(\hat{\mathbf{k}}) = \delta_{nn'}\delta_{mm'}\delta_{\mathbf{AB}}, \qquad \text{(A 3)}$$

and $\mathbf{A}$ and $\mathbf{B}$ can be any one of $\mathbf{Y}$, $\mathbf{X}$ or $\mathbf{Z}$.

The (outgoing) normalized vector spherical waves are defined as

$$\mathbf{M}_{nm}(k\mathbf{r}) \equiv -h_n(kr)\mathbf{X}_{nm}(\hat{\mathbf{r}}), \qquad \text{(A 4}a\text{)}$$

$$\mathbf{N}_{nm}(k\mathbf{r}) \equiv \frac{1}{kr}\{[n(n+1)]^{1/2}h_n(kr)\mathbf{Y}_{nm}(\hat{\mathbf{r}}) + [krh_n(kr)]'\mathbf{Z}_{nm}(\hat{\mathbf{r}})\}, \qquad \text{(A 4}b\text{)}$$

where h_n are the spherical Hankel functions of the first kind. The regular spherical waves are denoted by $\mathcal{R}g\{\mathbf{M}\}$ and $\mathcal{R}g\{\mathbf{N}\}$ and obtained by replacing the h_n in equations (A 4) with spherical Bessel fuctions j_n.

Appendix B. The vector wave addition theorem

This theorem involves infinite summations over the multipolarity numbers, $n = 1, 2, \ldots, \infty$ and $-n \leqslant m \leqslant n$. It therefore proves useful to define a generalized index $l \equiv n(n+1) - m$ for which each integral value of l corresponds to unique physical n, m pair [7]. One can then arrange the spherical wave components in an infinite column vector $\boldsymbol{\mathcal{E}}(k\mathbf{r})$, which will be truncated in numerical applications at some finite orbital multipolarity $n_{\max}(L_{\max} = n_{\max}^2 + 2n_{\max})$:

$$\boldsymbol{\mathcal{E}}(k\mathbf{r}) \equiv \begin{bmatrix}\mathbf{M}(k\mathbf{r})\\ \mathbf{N}(k\mathbf{r})\end{bmatrix} = \begin{bmatrix}\mathbf{M}_1(k\mathbf{r})\\ \vdots\\ \mathbf{M}_{L_{\max}}(k\mathbf{r})\\ \mathbf{N}_1(k\mathbf{r})\\ \vdots\\ \mathbf{N}_{L_{\max}}(k\mathbf{r})\end{bmatrix}. \qquad \text{(B 1)}$$

The addition theorem permits the transformation of spherical waves centred around a given point to be expressed in terms of spherical waves developed about a different origin. To be precise, let us consider a point P. Its spherical coordinate vector around an origin O is $\mathbf{r} = \mathrm{OP}$. Consider now another origin O′ for spherical coordinates with position vector $\mathbf{r}_0 = \mathrm{OO}'$. The spherical coordinates of P around this new origin are $\mathbf{r}' = \mathrm{O}'\mathrm{P} = \mathbf{r} - \mathbf{r}_0$.

Using the matrix notation of equation (B1) and taking the $L_{\max} \to \infty$ limit, the translation addition theorem [3, 7] of Stein [14] and Cruzan [15] expresses the spherical waves in the O coordinate system in terms of spherical waves in the O′ coordinate system:

$$\begin{aligned} \boldsymbol{\mathcal{E}}^{\mathrm{t}}(k\mathbf{r}) &= \boldsymbol{\mathcal{E}}^{\mathrm{t}}(k\mathbf{r}') \cdot \boldsymbol{\beta}(k\mathbf{r}_0), & r' > r_0, \\ \boldsymbol{\mathcal{E}}^{\mathrm{t}}(k\mathbf{r}) &= \mathcal{R}g\,\{\boldsymbol{\mathcal{E}}^{\mathrm{t}}(k\mathbf{r}')\} \cdot \boldsymbol{\alpha}(k\mathbf{r}_0), & r' < r_0, \\ \mathcal{R}g\,\{\boldsymbol{\mathcal{E}}^{\mathrm{t}}(k\mathbf{r})\} &= \mathcal{R}g\,\{\boldsymbol{\mathcal{E}}^{\mathrm{t}}(k\mathbf{r}')\} \cdot \boldsymbol{\beta}(k\mathbf{r}_0), & \forall |\mathbf{r}|. \end{aligned} \tag{B 2}$$

The symbols $\boldsymbol{\alpha}(k\mathbf{r}_0)$ and $\boldsymbol{\beta}(k\mathbf{r}_0)$ denote the irregular and regular translation–addition matrices respectively. The superscript t means that we have transposed a column vector into a row vector, and the dots (·) indicate that we have made a matrix multiplication over the spherical wave components. The *normalized* $\boldsymbol{\alpha}(k\mathbf{r}_0)$ and $\boldsymbol{\beta}(k\mathbf{r}_0)$ that we use have the form

$$\boldsymbol{\alpha}(k\mathbf{r}_0) = \begin{bmatrix} \bar{\mathbf{A}}(k\mathbf{r}_0) & \bar{\mathbf{B}}(k\mathbf{r}_0) \\ \bar{\mathbf{B}}(k\mathbf{r}_0) & \bar{\mathbf{A}}(k\mathbf{r})_0 \end{bmatrix}, \qquad \boldsymbol{\beta}(k\mathbf{r}_0) = \mathcal{R}g\,\{\boldsymbol{\alpha}(k\mathbf{r}_0)\}, \tag{B 3}$$

Closed forms for the matrix elements $A_{\nu\mu,nm}$ and $B_{\nu\mu,nm}$ were derived by Cruzan [15]. For extensive numerical calculations, we found it more efficient to express the *normalized* vector translation–addition coefficients in terms of the normalized scalar coefficients in the manner derived by Mackowski [5]. In the normalized convention [7, 13], these are

$$\begin{aligned} \bar{A}_{\nu,\mu;n,m} = \frac{1}{2}\left(\frac{1}{\nu(\nu+1)n(n+1)}\right)^{1/2} & [2\mu m \bar{\alpha}^{\mathrm{s}}_{\nu,\mu;n,m} \\ & + [(n-m)(n+m+1)]^{1/2}[(\nu-\mu)(\nu+\mu+1)]^{1/2}\bar{\alpha}^{\mathrm{s}}_{\nu,\mu+1;n,m+1} \\ & + [(n+m)(n-m+1)]^{1/2}[(\nu+\mu)(\nu-\mu+1)]^{1/2}\bar{\alpha}^{\mathrm{s}}_{\nu,\mu-1;n,m-1}], \end{aligned} \tag{B 4}$$

$$\begin{aligned} \bar{B}_{\nu,\mu;n,m} = -\mathrm{i}\frac{1}{2}\left(\frac{2\nu+1}{2\nu-1}\frac{1}{\nu(\nu+1)n(n+1)}\right)^{1/2} & \{2m[(\nu-\mu)(\nu+\mu)]^{1/2}\bar{\alpha}^{\mathrm{s}}_{\nu-1,\mu;n,m} \\ & + [(n-m)(n+m+1)]^{1/2}[(\nu-\mu)(\nu-\mu-1)]^{1/2}\bar{\alpha}^{\mathrm{s}}_{\nu-1,\mu+1;n,m+1} \\ & - [(n+m)]^{1/2}[(n-m+1)]^{1/2}[(\nu+\mu)(\nu+\mu-1)]^{1/2}\bar{\alpha}^{\mathrm{s}}_{\nu-1,\mu-1;n,m-1}\}, \end{aligned} \tag{B 5}$$

where $\bar{\boldsymbol{\alpha}}^{\mathrm{s}}$ are the normalized scalar translation–addition coefficients of appendix C below.

A significant mathematical advantage of the normalized convention for the spherical waves is that the complex conjugation of the regular translation matrices corresponds simply to inverse translation, that is

$$[\boldsymbol{\beta}(k\mathbf{r}_0)]^\dagger = \boldsymbol{\beta}(-k\mathbf{r}_0). \tag{B 6}$$

Appendix C. Scalar translation–addition coefficients

In appendix B, we gave expressions for the vector coefficient expressed in terms of normalized scalar coefficients. The normalized $\bar{\boldsymbol{\alpha}}^{\mathrm{s}}$ and $\bar{\boldsymbol{\beta}}^{\mathrm{s}}$ coefficients can be derived from recursion relations of the form [16]

$$\begin{aligned} a^+_{n-1,m}\bar{\alpha}^{\mathrm{s}}_{\nu\mu,nm} &= -a^-_{n-1,m}\bar{\alpha}^{\mathrm{s}}_{\nu\mu;n-2,m} + a^+_{\nu-1,\mu}\bar{\alpha}^{\mathrm{s}}_{\nu-1,\mu;n-1,m} + a^-_{\nu+1;\mu}\bar{\alpha}^{\mathbf{s}}_{\nu+1,\mu;n-1,m}, \\ b^+_{n-1,n-1}\bar{\alpha}^{\mathrm{s}}_{\nu\mu,nn} &= b^+_{\nu-1,\mu-1}\bar{\alpha}^{\mathrm{s}}_{\nu-1,\mu-1;n-1,n-1} + b^-_{\nu+1,\mu-1}\bar{\alpha}^{\mathrm{s}}_{\nu+1,\mu-1;n-1,n-1}, \end{aligned} \tag{C 1}$$

and likewise for $\bar{\boldsymbol{\beta}}^{\mathrm{s}}$. The coefficients $a^{\pm}$ and $b^{\pm}$ are given by

$$\begin{aligned} a^+_{nm} &= -\left[\frac{(n+m+1)(n-m+1)}{(2n+1)(2n+3)}\right]^{1/2}, \quad a^-_{nm} = \left[\frac{(n+m)(n-m)}{(2n+1)(2n-1)}\right]^{1/2}, \\ b^+_{nm} &= \left[\frac{(n+m+2)(n+m+1)}{(2n+1)(2n+3)}\right]^{1/2}, \quad b^-_{nm} = \left[\frac{(n-m)(n-m-1)}{(2n+1)(2n-1)}\right]^{1/2}. \end{aligned} \tag{C 2}$$

The recursion is initiated by

$$\begin{aligned} \bar{\beta}^{\mathrm{s}}_{\nu\mu,00} &= (4\pi)^{1/2}(-1)^{\nu+\mu}\, Y_{\nu,-\mu}(\theta_0,\phi_0) j_\nu(kr_0), \\ \bar{\alpha}^{\mathrm{s}}_{\nu\mu,00} &= (4\pi)^{1/2}(-1)^{\nu+\mu}\, Y_{\nu,-\mu}(\theta_0,\phi_0) h_\nu(kr_0). \end{aligned} \tag{C 3}$$

Negative values for m are evaluated by using the relations

$$\begin{aligned} \bar{\beta}^{\mathrm{s}}_{\nu\mu,nm}(x,\theta,\phi) &= (-1)^{\mu+m}\bar{\beta}^{\mathrm{s}*}_{\nu-\mu,n-m}(x,^*,\theta,\phi), \\ \bar{\alpha}^{\mathrm{s}}_{\nu\mu,nm}(x,\theta,\phi) &= -(-1)^{n+\nu+\mu+m}\bar{\alpha}^{\mathrm{s}*}_{\nu-\mu,n-m}(-x^*,\theta,\phi). \end{aligned} \tag{C 4}$$

References

[1] Wiscombe, W. J., 1980, *Appl. Optics*, **19,** 1505.
[2] Mackowski, D. W., 1991, *Proc. R. Soc.*, A, **433,** 599.
[3] Chew, W. C., 1994, *Waves and Fields in Inhomogeneous Media*, IEEE Press Series on Electromagnetic Waves (New York: IEEE Press).
[4] Siqueira, P. R., and Sarabandi, K., 2000, *IEEE Trans. Antennas Propagation*, **48,** 317.
[5] Mackowski, D. W., 1994, *J. Opt. Soc. Am.* A, **11,** 2851.
[6] Tzeng, Y. C., and Fung, A. K., 1994, *J. Electron Waves Applic.*, **8,** 61.
[7] Tsang, L., Kong, J. A., and Shin, R. T., 1985, *Theory of Microwave Remote Sensing*, Wiley Series in Remote Sensing (New York: Wiley).
[8] Mie, G., 1908, *Ann. In Deutsch. Physik*, **25,** 377.
[9] Bohren, C. F., and Huffman, D. R., 1983, *Absorption and Scattering of Light by Small Particles* (New York: Wiley–Interscience).

[10] Van de Hulst, H. C., 1981, *Light Scattering by small Particles* (New York: Dover Publications).
[11] Mackowski, D. W., and Miscshenko, M. I., 1996, *J. opt. Soc. Am.*, **13,** 2266.
[12] Bruning, J., and Lo, Y. T., 1971, *IEEE Trans. Antennas Propagation*, **19,** 378.
[13] Stout, B., Auger, J. C., and Lafait, J., 2001, *J. mod. Optics*, **48,** 2105.
[14] Stein, S., 1961, *Q. appl. Math.*, **19,** 15.
[15] Cruzan, O. R., 1962, *Q. appl. Math.*, **20,** 33.
[16] Chew, W. C., 1992, *J. Electron Waves Applic.*, **6,** 133.